

# Material-driven mesh derived from medical images. A case study on patient-specific modeling of the lumbar spine

H-Q.Nguyen<sup>1</sup>, M.Benoit<sup>1</sup>, C.Robin<sup>1</sup>, T-T.Dao<sup>1</sup>, A.Rassineux<sup>2</sup>, M-C.Ho Ba Tho<sup>1</sup>

<sup>1</sup>BMBI, <sup>2</sup>Roberval, University of Technology of Compiègne, France, { ho-quang.nguyen, tien-tuan.dao, alain.rassineux, marie-christine.ho-ba-tho}@utc.fr, { caroline.jobin, marc.benoit}@etu.utc.fr

---

**Resume** — This work presents a methodology for patient-specific finite element modeling which takes both individualized geometry and material properties of biological structures into consideration. In this study, the mesh is driven by personalized material knowledge which is extracted from advanced medical imaging. Additionally, a user-friendly program including image processing, material-driven meshing and material properties assignment, named C3M “Computed Material-driven Mesh Model”, has been developed to generate efficiently subject-specific FE models derived from medical images. This process is applied to generate a patient specific FE model of lumbar spine based on both MRI and CT images.

**Keywords** — patient specific finite element model; material-driven meshing; medical images; lumbar spine

---

## 1. Introduction

Low back pain is a common health problem which impacts a large part of the population in industrialized countries. Over the years, numerical modeling has been widely studied to investigate the biomechanics of lumbar spine for strongly assisting clinicians in diagnosis and treatments of this spinal pathology. In recent years, there has been a growing interest in researching and developing patient specific computer modelling which has proven its ability to provide great promises for inferring realistic model of individual subject. However, still the specificity of these models is not fully described or is limited to patient geometry. In fact, few models consider appropriate material properties derived from tissue characterization obtained from medical images. Furthermore, patient specific models can be obtained with geometry and mechanical properties derived from CT, but few from MRI which is well-suited for examining soft tissues. Therefore, development of the high-fidelity, patient-specific finite element model of the lumbar spine still presents the challenge. In this context of patient-specific finite element modeling, mesh generation is a crucial issue which requires an accurate representation of the geometry with well-shaped and sized elements and a relevant distribution of materials.

In the framework of patient-specific finite element modeling of the lumbar spine, there is lack of exploitation of both MRI and CT to derive the model which takes both personalized geometry and material into consideration simultaneously. Additionally, there is no fully integrated process for geometric modeling, material-driven mesh and material assignment of the spinal structures in which the mesh is driven by material properties from medical images. In fact, the purpose of this study is to provide solutions for this modeling challenge.

Therefore, the objective of this work is to develop a new strategy to create patient specific finite element models by integrating material knowledge for driving the meshing process. An integrative modelling workflow, including an easy-to-implement segmentation method, a material-driven meshing process based on an efficient mesh generator and material properties assignment process is proposed to create high fidelity finite element models of the lumbar spine from both MRI and CT images.

## 2. Materials and methods

### 2.1. Computational workflow

An integrative modeling workflow including image processing, meshing, material properties assignment is developed (Figure 1). Each component of this workflow is described in the following subsections.

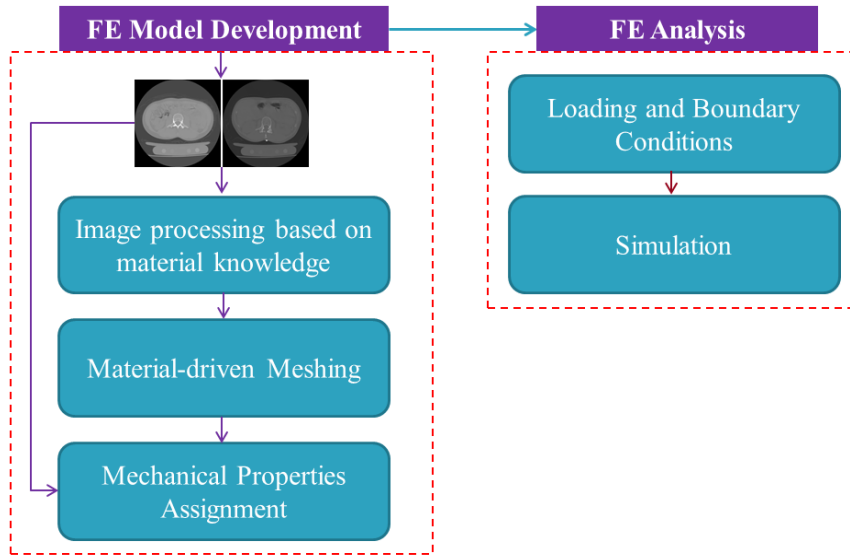


Figure 1 – Modeling workflow

### 2.2. Image processing based on material properties knowledge

The aim of the first stage of the finite element model development is to define different regions in the tissues from medical images. In this process, a semi-automatic segmentation coupled with a threshold process based on material knowledge is developed to obtain multi-level masks which represent the heterogeneity of the material.

In the first step of this process, the semi-auto segmentation is performed to extract the tissue's boundary and output a set of binary masks. This step is based on two alternative methods: Canny method [1] and fast continuous max-flow approach [2]. The former technique is used due to its easy implementation while the latter technique is more complex and computationally expensive, but can efficiently provide more accurate results.

The Canny method is implemented to find edges by looking for local maxima of the gradient of image associated with a Gaussian filter. There are two thresholds related to the Canny algorithm: a highest threshold of the gradient magnitude of the image for selecting strong edges, and a low threshold (i.e.  $0.4 \times \text{high threshold}$ ) for selecting weak edges which are connected to strong edges. Note that, in this study, the high threshold value is calculated by using the Otsu algorithm (Otsu 1979) which is a well-known method of choosing threshold value automatically. Additionally, the post-processing is automatically performed to remove small objects with minimal number pixels criteria from binary image. Finally, labelled masks in binary are generated.

The other alternative technique implementing in this step is new continuous max-flow algorithm which was developed by Yuan et al. (2010) for efficiently solving the continuous min-cut problems. The maximal flow problem is to find the largest amount of flow allowed to pass from the source  $s$  to the sink  $t$  without violating any capacity constraint. It should be note that the source and sink related

to background and foreground is determined based on Otsu threshold. Therefore, there is no manual selection for the source and the sink in this case. Additionally, the auto-segmentation is also improved by considering the 3D pixel connectivity with 6-connected background neighbors in 3D view (axial, sagittal, coronal plane) to avoid or limit artifacts, such as holes.

The second step of this process is multi-level mask generation. Based on material property knowledge for inhomogeneous biological tissues, the appropriate threshold values are chosen to establish multi-level masks representing the multi-material regions of the tissue. The material property knowledge, for instance, can be derived from bone characterization for vertebrae [3, 4] or tissue-based data from advanced MRI protocols for IVDs [5, 6].

### **2.3. Material-driven mesh generation**

A specific material-driven meshing process is developed based on an open-source mesh generator Iso2mesh V1.7.9 2013 [7]. From multi-level 3D images, a multi-domain 3D mesh is directly generated using 'vol2mesh' utility of Iso2mesh with constrained Delaunay tetrahedralisation (CDT) extraction method. It should be highlighted that interfaces of multi-domain are defined by material knowledge via the multi-level mask.

To estimate the shape quality of the material-driven meshed model, Joe-Liu index [8] is used. The index value closed to one indicates higher mesh quality (equilateral tetrahedron) and a value closed to 0 means nearly degenerated element, flat or elongated.

### **2.4. Material properties assignment**

The in vivo quantitative information of tissues which characterizes biomechanical behavior of the tissues can be extracted directly from medical images (CT, MRI) and then assigned to the models for FE analysis.

Regarding the bone tissue, it is well known that its mechanical properties can be derived from CT images due to the high contrast between the bone tissue and the soft tissues around in CT images as well as the linear correlation between CT numbers and apparent density of biologic tissues. In the first step of material properties assignment, by using the numerical integration method [9], the material mapping is implemented to assign the average of CT numbers to relevant elements of the material-driven volume mesh. The CT value assigned to each node is approximately equivalent to the CT value of the voxel enclosing that node.

After that, depending on which region the element belongs to, relevant correlations established in literature study [3, 4] are adequately applied to convert the CT value of that element to density and elastic modulus values. This procedure can provide different material distribution for each mesh element which results in a good representation of the inhomogeneity, however, leads to the computational problems. In fact, the number of materials can be reduced by separating the whole range of material values into material cards by a  $\Delta E$  threshold.

With respect to the soft tissues, like intervertebral disc (IVD), the same process is applied to assign material properties to mesh model. However, the biomechanical behaviour is derived from advanced Magnetic Resonance Imaging sequences such as T2 mapping, diffusion-weighted and diffusion tensor sequences [5, 6].

## **2.5. A case study- Patient-specific finite element model of lumbar spine with material-driven mesh derived from CT and MRI images**

### **2.5.1. Lumbar spine modeling derived from CT and conventional MRI data**

To test our developed modelling workflow, the finite element model of a whole lumbar spine is generated. The dataset consisting of 343 CT images and 19 sagittal T2-weighted MR images of a patient are obtained from the MYSPINE European project. The CT and MRI images have the voxel resolution of  $0.607 \times 0.607 \times 1.25 \text{ mm}^3$  and  $0.7 \times 0.7 \times 3.0 \text{ mm}^3$ , respectively.

The FE models of vertebrae are generated by implementing the integrative modeling process C3M. Accordingly, a multi-label dataset representing not only cortical bone, spongy bone but also facet joints and endplates is firstly obtained by performing the image processing based on material knowledge derived from CT [3, 4]. After that, from this dataset, a multi-material mesh is generated by using Iso2mesh function. The same process is applied to generate a FE model of IVD. In this case, the multi-label dataset including both annulus fibrosus (AF) and nucleus pulposus (NP) is derived from the conventional MRI images. In order to facilitate the assembly of vertebrae and IVD, the MRI-based IVD mesh is non-rigidly aligned to an CT-based IVD mesh based on iterative closest point (ICP) algorithm. In order to test the quality of meshed models, the FE analysis is performed on model. Mooney-Rivlin hyperelastic material constants reported in [10] are used to model the mechanical behavior of the IVD. For the boundary conditions, the model is submitted to a finite element analysis with an axial compressive load of 1000 N on L1 with a distribution of 80% of load for the upper endplate, 10% of load for the left upper facet joint and 10% of load for the right upper facet joint. All the nodes from the lower endplate of the vertebra L5 are constrained in all directions. All the interfaces between endplates and between facet joints are defined as tied contacts.

### **2.5.2. IVD modeling derived from advanced MRI data**

This subsection aims at developing the patient-specific model of IVD from advanced MRI data by using the proposed C3M software. In this work, the material knowledge of IVD is the quantitative information on NP and AF, such as T2 relaxation time, the apparent diffusion coefficient (ADC), which is derived from T2 mapping, diffusion-weighted and diffusion tensor MR imaging.

Basically, the same process for vertebrae modeling, which is detailed in aforementioned subsection 2.6.1, is applied for IVD modeling. Firstly, from the T2 weighted-MRI images, the outer of the IVD is defined and represented as binary masks by implementing semi-auto segmentation process in C3M software. Subsequently, multi-label masks representing the AF and 2 regions of NP are obtained based on material properties knowledge which is in this case tissue-based data from advanced MRI protocols [5]. In this step, the T2 mapping are used to derive the multi-level masks. The T2 values are mapped into the binary masks which define the outer of IVD. After that, two thresholds  $t_1$ ,  $t_2$  are chosen based on [5] and applied to this T2 map of the segmented images in order to generate the multi-level masks which represent different regions in the IVD. After that, the multi-region mesh is generated from the multi-label dataset. And finally, biochemical properties quantified from advanced MRI protocols are assigned to the model. In this step, both T2 and ADC maps are used to characterize the material of IVD model. It should be noted that T2-mapping has been used to quantify the changes in water contents of disc composition through T2 relaxation time property. While ADC map provides a quantitative analysis of the motion (direction and magnitude) of proteoglycan and water molecules. In this study, the water content, glycosaminoglycans (GAGs) per (dry weight) are considered and deduced from following empirical linear regression [5, 6].

### 3. Results and discussions

Results of the generation of patient-specific lumbar spine model are illustrated in Figure 2.

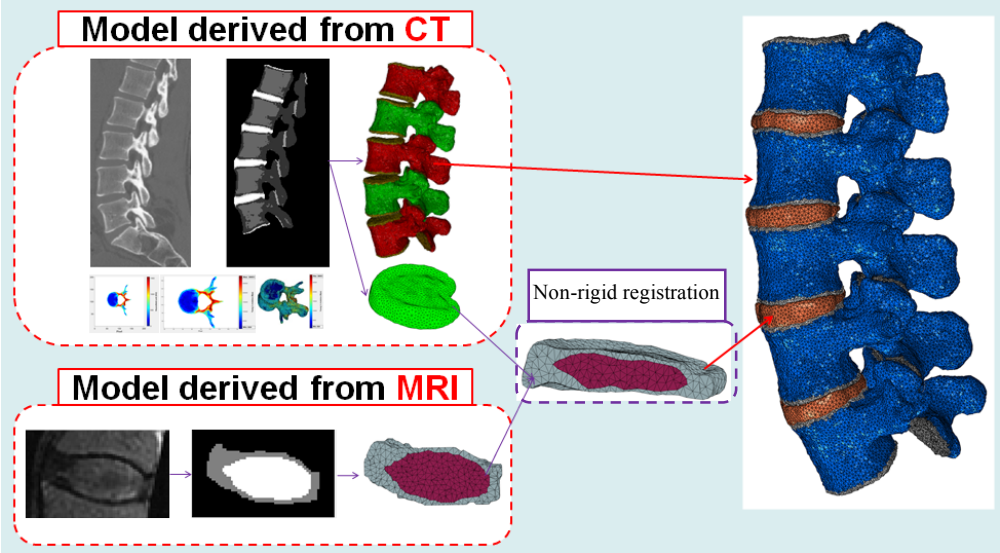


Figure 2 - The generation of patient-specific lumbar spine model

One can observe similarity between distribution of CT values (Figure 3a) on segmented CT images with that of cross section of 3D mesh material driven (Figure 3c).

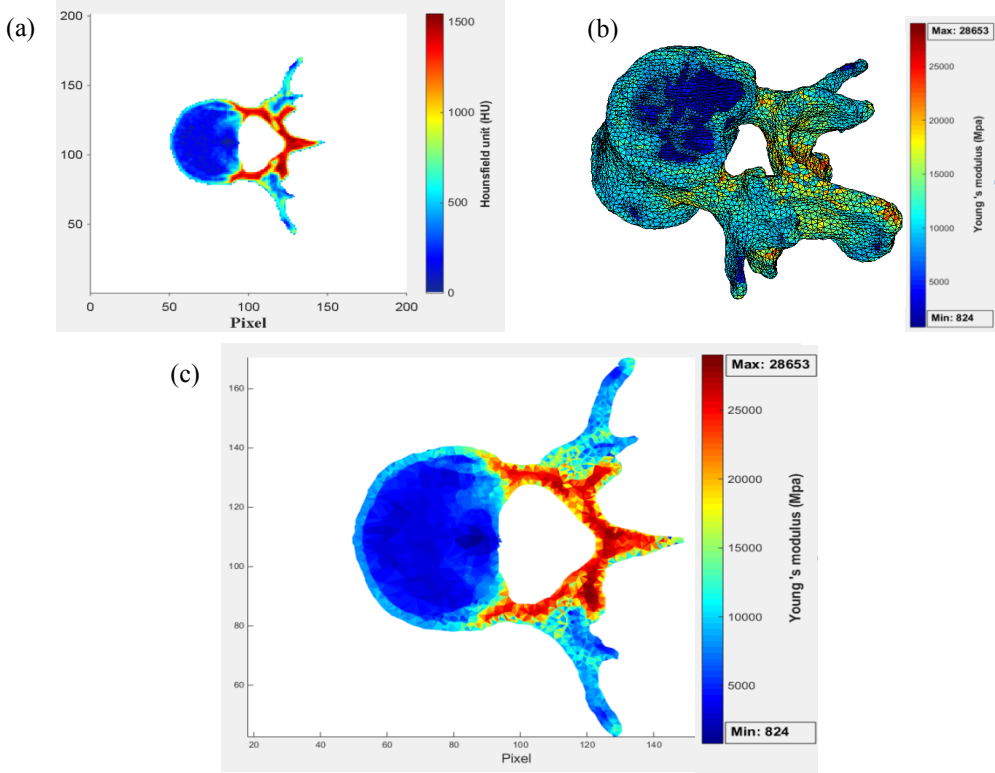


Figure 3 –Material distributions on segmented CT slices (a), material-driven meshes (b) and cross sections with Young’s modulus mapping (c)

The FEA results are shown in Figure 4. Compared to the other studies in literature [10], the simulation outcomes are in the range of expected values.

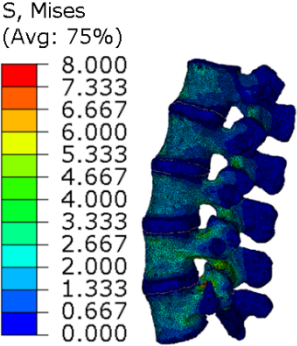


Figure 4 – FEA result of the lumbar spine without sacrum

Figure 5 illustrates the results of material-driven mesh generation of IVD derived from T2 mapping.

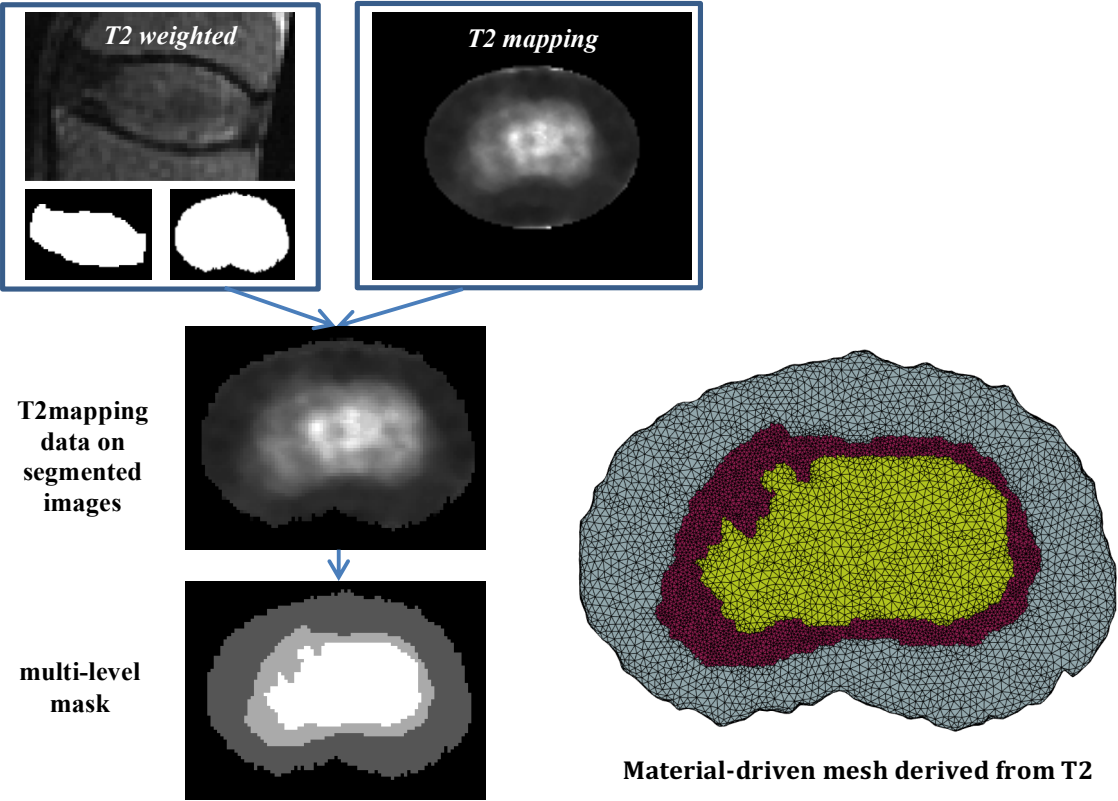


Figure 5 –Material-driven mesh generation of IVD derived from T2 mapping

Figure 6 illustrates the material-driven mesh derived from T2 map with the distribution of T2 relaxation time visualized at the cross section of IVD. Then the distribution of biochemical properties derived from advanced MRI data such as water content and GAG/dry weight can be used from our work [5, 6].



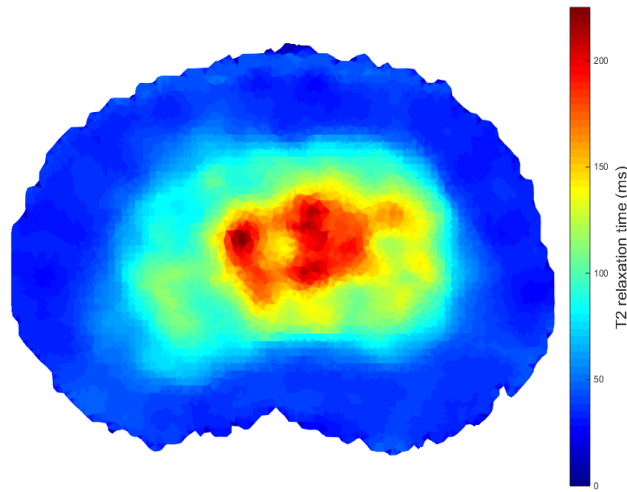


Figure 6. Distribution of T2 relaxation time visualized at the cross section of the IVD model.

To the best of our knowledge, the proposed finite element model of the lumbar spine (vertebrae and IVD) is the first patient specific FE model with meshed model generated using material knowledge derived from CT and MRI images. The proposed model allows an accurate and straightforward assembly of vertebrae and IVDs considering both geometry and material properties reflecting patient-specificity. Especially, the proposed IVD model which is derived from T2 mapping takes both individualized geometry and materials into consideration. This model can be seen as the first IVD mesh model composed of 3 distinguished personalized regions including AF, outer and inner NP. Additionally, the patient-specific quantitative information on IVD, such as water content, GAGs can be included in this proposed model by means of T2 and ADC mapping. This can open the way for biomechanical modeling in daily life activities.

This method presents a new approach for lumbar spine modelling and outperforms the general procedure used in literature. Indeed, instead of using different specific commercial software for different tasks of lumbar spine modeling, this study implements the proposed C3M software, which is a fully integrated process of geometry modeling, material-driven mesh, material properties assignment, in order to generate the model more straightforwardly. Moreover, unlike conventional approaches which need to perform 3D geometry reconstruction before 3D mesh generation, the proposed approach can directly generate 3D mesh from medical images. In this study, Canny method is used due to its easy implementation while the continuous max-flow algorithm is more complex and computationally expensive, but can efficiently provide more accurate results. Concerning the meshing, Iso2mesh was selected because it is easy-to-use and its implementation is compatible with other components of our proposed workflow. In particular, Iso2mesh is capable of dealing with open-surface problems and controlling mesh density. The benchmarking has been done and shows that our software C3M is twice faster than commercial software, furthermore material distribution integration is automatically included in the models generated by C3M. Compared to statistical models, our software C3M is slower in terms of the time processing but has more subject specific data including both geometry and material properties.

#### 4. Conclusions and perspectives

This study presents a methodology for patient-specific finite element modelling which takes both individualized geometry and material properties of biological structures into consideration. More

specifically, in this study, the mesh model is driven by personalized material knowledge which is extracted from advanced medical imaging. This approach opens a new direction to improve the meshing process using material knowledge derived from medical images. Perspective work relates to the application of the proposed method for a patient cohort.

## 5. Acknowledgements

The authors would like to thank the Collegium UTC-CNRS INSIS for their financial support and MySpine European Consortium for their collaboration.

## References

- [1] J. Canny .A Computational Approach to Edge Detection. IEEE Transactions on Pattern Analysis and Machine Intelligence PAMI 8 (6), page 679-page 698, 1986.
- [2] J. Yuan, E. Bae, XC. Tai. A study on continuous max-flow and min-cut approaches. In: Proceedings of IEEE Conference on Computer Vision and Pattern Recognition; 2010 June 13-18; San Francisco, USA. CVPR 2010, page 2217– page 2224, 2010.
- [3] MC. Ho Ba Tho, JY. Rho, RB. Ashman. Atlas of mechanical properties of human cortical and cancellous bone. In: Van der Perre G., Lowet A (eds), In vivo assessment of bone quality by vibration and wave propagation techniques, Part II, ACCO press, Leuven, page 1–page 38, 1992.
- [4] MC. Ho Ba Tho. Bone and joints with individualised geometric and mechanical properties derived from medical images, Computer Mechanics and Engineering Sciences 4 (3-4), page 489-page 496, 2003.
- [5] TT. Dao, P. Pouletaut, L. Robert, P. Aupaure, F. Charleux, MC. Ho Ba Tho. Quantitative Analysis of Annulus Fibrosus and Nucleus Pulposus derived from T2 Mapping, Diffusion-weighted and Diffusion Tensor MR Imaging, Computer Methods in Biomechanics and Biomedical Engineering: Imaging & Visualization 1(3), page138-page146, 2013.
- [6] J. Noailly, TT. Dao, MV. Rijsbergen, A. Bonet, P. Pouletaut, F. Charleux, K. Ito, MC. Ho Ba Tho, Theoretical discrimination between intra- and extra-fibrillar water improves experimental correlations between intervertebral disc qMRI and composition, In: 6th International Conferene on Computational Bioengineering, ICCB2015 Barcelona, Spain, September 14-16, 2015.
- [7] Q. Fang and D. Boas. Tetrahedral mesh generation from volumetric binary and gray-scale images. Proceedings of IEEE International Symposium on Biomedical Imaging: From Nano to Macro 2009, page 1142-page 1145, 2009.
- [8] A. Liu and B. Joe. Relationship between tetrahedron shape measures. BIT Numerical Mathematics 34 (2), page 268-page 287, 1994.
- [9] F. Taddei, A. Pancanti, M. Viceconti. An improved method for the automatic mapping of computed tomography numbers onto finite element models, Med. Eng. & Phys 26(1), page 61–page 69, 2004.
- [10] E. Ibarz, A. Herrera, Y. Más, J. Rodríguez-Vela, J. Cegoñino, S. Puértolas, and L. Gracia. Development and Kinematic Verification of a Finite Element Model for the Lumbar Spine : Application to Disc Degeneration, BioMed Research International 2013, page 1– page 18, 2013.